COBEM 2021 26th International Congress of Mechanical Engineering
November 22-26, 2021, Virtual Congress, Brazil

COB-2021-0585
A WIDE-BAND FORMULATION FOR THE WEIGHTED-SUM-OF-GRAY-GASES MODEL APPLIED TO NON-ISOTHERMAL PARTICIPATING MEDIA

Roberta Juliana Collet da Fonseca
Guilherme Crivelli Fraga
Felipe Ramos Coelho
Francis Henrique Ramos França
Department of Mechanical Engineering, Federal University of Rio Grande do Sul, Porto Alegre, Brazil
roberta.fonseca@ufrgs.br
guilhermecfraga@ufrgs.br
felipe.coelho@ufrgs.br
frfranca@mecanica.ufrgs.br

Abstract. *Thermal radiation contributes greatly to the heat transfer in combustion systems due to the high temperatures. However, the correct prediction of the radiation requires a detailed knowledge of the absorption coefficient of the participating gases, which presents a strongly irregular behavior with the wavenumber. Global spectral models, such as the weighted-sum-of-gray-gas (WSGG) model, present an alternative to the spectral integration of the radiative transfer equation (RTE) with low computational effort and good accuracy when compared to the line-by-line (LBL) integration. In this framework, this paper proposes a methodology for generating correlations for participating species, in which the spectrum is partitioned into a set of regions and the WSGG model is used to solve each spectral interval. The emittances are obtained from LBL calculations for each spectral range, and the pressure-absorption coefficients and temperature coefficients of the WSGG model are obtained for each gray gas. These correlations are tested for non-coupled, radiative transfer calculations and compared to the LBL integration. The results obtained with the proposed method show a reduction of up to a third in deviations from the LBL solution compared to the performance of other formulations of the WSGG model.*

Keywords: *radiative transfer, participating gases, weighted-sum-of-gray-gases model, line-by-line integration, spectral intervals*

1. INTRODUCTION

The growing environmental concern in reducing the use of fossil fuels and the emission of pollutants into the atmosphere makes even more necessary the development of accurate computational methods that provide a high-fidelity modeling of the heat transfer by thermal radiation, which cannot be neglected in combustion applications, since the chemical reactions occur at elevated temperatures. Nonetheless, the modeling of the thermal radiation in participating gases is a challenging task due to the highly complex behavior of the absorption coefficient of each chemical species involved, which varies greatly with the wavenumber. Although the line-by-line (LBL) integration (Taine, 1983) provides a highly accurate solution of the radiative transfer equation (RTE), its calculation is often impractical due to the elevated computational cost required to account for the hundreds of thousands of lines — extracted from the high resolution spectroscopic databases, such as HITEMP (Rothman *et al.*, 2010) and HITRAN (Gordon *et al.*, 2017) — that describe the behavior of the absorption coefficient of the gas on the radiation spectrum. In this framework, the development of accurate and efficient global gas models for solving the spectral integration of the radiative heat transfer is one of the most important areas in the thermal radiation field.

The simplest approach of the spectral models is the gray gas (GG) model, in which the absorption coefficient is assumed to be uniform over the spectrum, being independent of the wavenumber. This assumption simplifies the spectral behavior of the absorption coefficient of the gases, which consequently leads to inaccuracies in the prediction of the radiative transfer in participating media. However, the GG model has shown to be suitable to solve problems with high soot concentration (Mossi *et al.*, 2012; Cassol *et al.*, 2015; Fraga *et al.*, 2019).

Among the global models that do not require great detail of spectral data and, therefore, approximate the radiative properties considering the totality of the spectrum at once, there is the weighted-sum-of-gray-gases (WSGG) model (Hottel and Sarofim, 1967), which presents an alternative to the spectral integration of the RTE with low computational effort and a satisfactory level of accuracy when compared to the LBL benchmark solution. In short, the WSGG model replaces the highly irregular behavior of the absorption coefficient of a participating species by a small number of gray gases with uniform

absorption coefficient and transparent windows. Each gray gas has a weighting absorption coefficient, which is determined by fitting the values of total emittance calculated from spectral databases. Despite being an old and simplified method, the WSGG model has undergone great evolution in the last years, presenting results as good as more advanced models for many applications and, consequently, it has been extensively studied by several authors recently (Kangwanpongpan *et al.*, 2012; Dorigon *et al.*, 2013; Cassol *et al.*, 2014; Brittes *et al.*, 2017; Coelho and França, 2017; Centeno *et al.*, 2018; Coelho and França, 2018; Wang and Xuan, 2019; Bordbar *et al.*, 2021; He *et al.*, 2021).

Although it is outside the scope of this paper, there are other more modern spectral models, such as the spectral line-based WSGG (SLW) model (Denison and Webb, 1993), the full-spectrum k (FSK) distribution (Modest and Zhang, 2000) and the cumulative wavenumber (CW) method (Solovjov and Webb, 2002). However, the WSGG model presents some advantages in relation to these other methods, as its simplicity and lower computational cost. In this framework, the present study proposes a new approach for determining the WSGG coefficients in which the gas emittance is not generated for the full spectrum, as in the standard methodology, but for a set of bands. The HITEMP 2010 database is employed to generate the absorption spectra of water vapor used to fit the model parameters. The new correlations are applicable to a range of path lengths, varying from 0.001 m to 30 m, for a total pressure of 1 atm and for non-isothermal and homogeneous conditions. To validate the model, the WSGG emittance for each spectral interval is compared to the LBL solution for temperatures ranging from 400 K to 2500 K. Furthermore, the accuracy of the correlations is also tested by comparing the results obtained for the radiative heat flux and radiative heat source with the LBL integration for the one-dimensional domain studied, which is composed of pure H_2O confined between two parallel and black plates.

2. RADIATION MODELING

For a participating medium for which the scattering effects are negligible, the energy balance for the radiative heat transfer is computed by the RTE, which is written as (Modest, 2013; Howell *et al.*, 2016)

$$\frac{\mathrm{d}I_\eta}{\mathrm{d}s} = -\kappa_\eta I_\eta + \kappa_\eta I_{b\eta}\,, \tag{1}$$

in which I_η is the spectral radiation intensity, κ_η is the spectral absorption coefficient of the medium and $I_{b\eta}$ is the blackbody spectral radiation intensity, obtained from the Planck's distribution function for a wavenumber η and a medium temperature T, along a given path.

2.1 The standard WSGG model

The global solution of the radiation heat transfer requires the integration of the RTE over the spectrum and all directions. In this paper, the directional integration is resolved with the discrete ordinates method (DOM) (Chandrasekhar, 1960) for 8 directions (Lathrop and Carlson, 1964). The spectral part is solved through the WSGG model (Hottel and Sarofim, 1967), which is a global spectral model in which the radiation spectrum is replaced by a set of gray gases where the absorption coefficients are uniform plus transparent windows (Modest, 2013; Howell *et al.*, 2016).

For the application of the WSGG model, it is required the determination of the pressure-absorption coefficients and the temperature dependent coefficients. These gas parameters are usually obtained by fitting global radiation data, such as the total emittance along a certain path distance in the medium at some given temperature and composition. So, in this framework, the starting point for obtaining the parameters for the WSGG model is to determine the total emittance of the medium along a given path of length S, which is defined as

$$\varepsilon = \frac{\int_{\eta=0}^{\infty} I_{b\eta}[1-\exp(-\kappa_{p\eta}p_a S)]\mathrm{d}\eta}{I_b}\,, \tag{2}$$

where p_a is the partial pressure of the absorbing-emitting species, $\kappa_{p\eta}$ is the pressure-absorption coefficient, which is given by $\kappa_{p\eta} = \kappa_\eta/p_a$, and I_b is the total blackbody intensity; the product $p_a S$ is the pressure path-length.

Integrating Eq. (2) over the spectrum under the assumptions of the WSGG model, the total emittance becomes

$$\varepsilon = \sum_{j=1}^{J} a_j[1-\exp(-\kappa_{pj}p_a S)]\,, \tag{3}$$

in which a_j is the temperature coefficient and κ_{pj} is the pressure-absorption coefficient, both for the gray gas j, which is assumed constant in each portion of the spectrum. The term a_j in the above equation represents the fraction of the total blackbody emission in the spectrum portion in which the absorption coefficient of the j-th gray gas is κ_{pj}. The total emittance in Eq. (2) can be calculated through LBL integration of the wavenumber spectrum for a set of temperatures T and pressure path-lengths $p_a S$. From that, Eq. (3) can be employed to fit values for pressure-absorption coefficients κ_{pj} and temperature coefficients a_j for each gray gas j.

Applying the WSGG model for a gray gas j to Eq. (1) leads to

$$\frac{\mathrm{d}I_j}{\mathrm{d}x} = -\kappa_{pj} p_a I_j + \kappa_{pj} p_a a_j I_b \,, \tag{4}$$

where I_j is the radiation intensity of the j-th gray gas. The total radiation intensity I can be computed by a summation of the partial intensities I_j related to each gray gas, such that $I = \sum_{j=1}^{J}$. The coefficient a_j, which is a weighting factor for the j-th gray gas, is frequently fitted as a polynomial function of temperature as

$$a_j = \sum_{k=0}^{J} b_{j,k} T_k \,, \tag{5}$$

in which $b_{j,k}$ are the k-th order polynomial coefficients of the gas j. The temperature dependent coefficient for the transparent windows is calculated as $a_0 = 1 - \sum_{j=1}^{J} a_j$, which assures that the energy is conserved.

Assuming a one-dimensional medium slab, as that is shown at the top left of Fig. 1, in which the participating medium is confined by two infinite parallel black walls separated by a distance L, the boundary conditions in the framework of the discrete ordinates method for an arbitrary direction l are given by: $I^{+}_{j,l,x=0} = a_{j,x=0} I_{b,x=0}$ and $I^{-}_{j,l,x=L} = a_{j,x=L} I_{b,x=L}$, in which $I^{+}_{j,l}$ and $I^{-}_{j,l}$ are the radiation intensities for gray gas j in the forward and backward directions, respectively, and $x = 0$ and $x = L$ are the left and right boundaries of the domain.

The radiative heat flux, q_r, and the radiative heat source, S_r, for the WSGG model are obtained by integrating Eq. (4) with the DOM for all directions and balancing the positive and negative intensities, such that

$$q_r(x) = \sum_{l=1}^{n_d} \sum_{j=1}^{J} 2\pi \mu_l \omega_l [I^{+}_{j,l}(x) - I^{-}_{j,l}(x)] \tag{6}$$

$$S_r(x) = \sum_{l=1}^{n_d} \sum_{j=1}^{J} 2\pi \omega_l \kappa_j [I^{+}_{j,l}(x) + I^{-}_{j,l}(x)] - 4\pi \kappa_j a_j I_b(x), \tag{7}$$

where κ_j is the absorption coefficient for the gray gas j ($\kappa_j = \kappa_{pj} \times p_a$), μ_l and ω_l are the cosine and the quadrature weight, both for direction l, and n_d is the number of directions used in the angular integration of the RTE.

2.2 The proposed model

In this study, a new approach for the weighted-sum-of-gray-gases model is presented, the wide-band based on WSGG (WBW) model. This spectral model consists of refining the spectrum by dividing it into several spectral intervals $\Delta\eta$ and applying the standard WSGG model to each one of these regions. Four gray gases are distributed in each spectral interval and the result is given by the summation of the contributions from each one of these segments. A similar implementation was proposed by Fonseca *et al.* (2020), in which a division of the spectrum into a set of bands was performed and the gray gas model was used to solve each one of the intervals. The same idea is used here, however, the method for the spectral integration of the RTE is the WSGG model. On the right side of Fig. 1, a comparison between κ_η of a participating gas for the LBL method and the WBW model for an arbitrary band $\Delta\eta$ is presented.

The first step in the generation of coefficients of the WBW model is to obtain the spectral lines that describe the behavior of the absorption coefficient of the participating gases involved. These spectral lines represent the distribution of the absorption cross-section as a function of wavenumber for a desired species and for a given temperature, total pressure and molar concentration, which are extracted from spectral databases such as HITEMP 2010 used in this paper. For instance, for water vapor, which is the chemical species under study in this paper, the absorption spectra required for the LBL solution are generated for a wavenumber range $0\,\mathrm{cm}^{-1} < \eta < 25\,000\,\mathrm{cm}^{-1}$, with the spectrum divided into 375 000 elements and a spectral resolution of $0.067\,\mathrm{cm}^{-1}$. The spectrum is divided into five spectral intervals following the methodology proposed in Marin and Buckius (1998), who developed correlations for the study of wide-bands models by using LBL data. The spectral ranges are described in Section 2.3.

From the absorption spectra, the values of emittance along any path-length can be determined through Eq. (2). However, as the spectrum is being divided into a set of bands, it is necessary to correct this equation in order to account for the fraction of blackbody energy emitted in that region of the spectrum, rather than calculating ε over the entire spectrum. Thus, for each spectral interval, the emittance is calculated as

$$\varepsilon = \frac{\int_{\Delta\eta} I_{b\eta} [1 - \exp(-\kappa_{p\eta} p_a S)] \mathrm{d}\eta}{f_{\Delta\eta} I_b} \,, \tag{8}$$

in which $f_{\Delta\eta}$ is the fraction of the blackbody energy emitted in the spectral interval $\Delta\eta$ and is given by $f_{\Delta\eta} = \int_{\Delta\eta} I_{b\eta} \mathrm{d}\eta / I_b$. Since the blackbody intensity is weighted by the fraction of blackbody energy, it is necessary to account for $f_{\Delta\eta}$ in the calculations of the RTE, boundary conditions, radiative heat flux and radiative heat source.

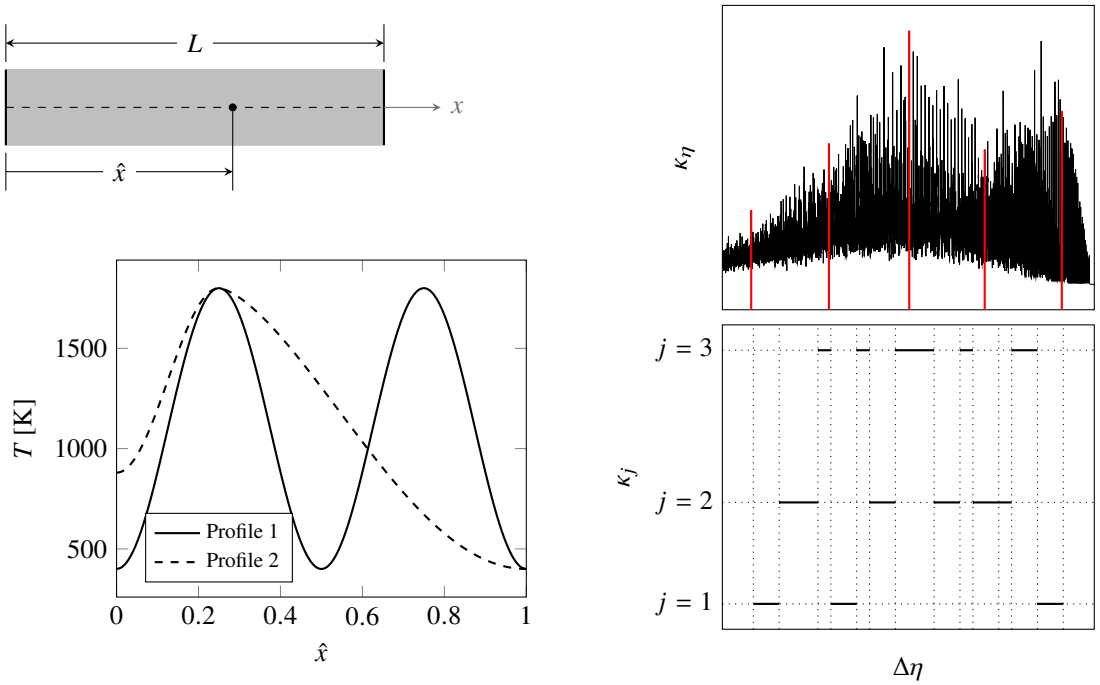

Figure 1. On the left: geometric representation of the one-dimensional domain (on the top); temperature profiles (at the bottom). On the right: schematic representation of the absorption coefficient for a participating gas and an interval $\Delta\eta$. κ_η for the LBL integration (on the top); κ_j for the WBW model (at the bottom).

In order to obtain the WBW coefficients for each spectral interval $\Delta\eta$, the procedure that has be followed is analogous to that performed to obtain κ_{pj} and a_j in the WSGG model. The Levenberg-Marquardt (LM) method (Marquardt, 1963) is used to fit these parameters through the commercial software Statistical Package for the Social Sciences (SPSS) 18 (IBM, 2016) based on LBL data computed via Eq. (8) calculated for a range of path-lengths and temperatures. For the simulations of this study, 43 values of path-lengths, varying from 0.001 m to 30 m, and 22 temperatures, between 400 K and 2500 K with intervals of 100 K, for each path-length are used to determine the WBW coefficients. Then, for each spectral interval $\Delta\eta$, the emittances are summed up for 22 temperatures T_m for each path-length according to

$$\sum_{m=1}^{M=22} \varepsilon_m(p_a S) = \sum_{j=1}^{J=4} \left[\sum_{m=1}^{M=22} a_j(T_m) \right] [1 - \exp(-\kappa_{pj} p_a S)] = \sum_{j=1}^{J=4} A_j [1 - \exp(-\kappa_{pj} p_a S)], \tag{9}$$

where m is the number of temperatures in which the emittances are calculated and A_j is the summation of the temperature coefficients a_j for all temperature range.

The adjustment is made by applying a non-linear multiple regression using the LM method to determine the absorption coefficients κ_{pj} from Eq. (9). From the coefficients κ_{pj}, one obtains the coefficients a_j by a new non-linear regression, again applying Eq. (9) for each one of 22 temperatures. The coefficients $b_{j,k}$ are obtained by a polynomial fit of the coefficients a_j as a function of the temperature according to Eq. (5), where the order of the polynomial function is equal to the number of gray gases ($j = k = 4$ in this paper). Finally, to validate the WBW correlations, new values of the emittances and coefficients are calculated through Eqs. (5) and (9) for each temperature and $p_a S$ and compared with the original values of ε obtained directly by LBL integration.

Since the spectrum is divided into $\Delta\eta$ spectral intervals, the WBW model is applied to each of these regions by accounting for the fraction of blackbody energy emitted at each band, so that a modification in the RTE is required. Thus, in the framework of the proposed method, for a given band i, Eq. (4) becomes

$$\frac{\mathrm{d}I_{j,i}}{\mathrm{d}x} = -\kappa_{pj,i} p_a I_{j,i} + \kappa_{pj,i} p_a a_{j,i} f_i I_b \,, \tag{10}$$

in which f_i is multiplied by the blackbody intensity I_b in order to weight the quantity of energy emitted in the i-th spectral interval.

Analogously to the RTE, the fraction of the blackbody energy emitted in each region in which the radiation spectrum is divided has to be accounted for in the boundary conditions. Thus, for the boundaries $x = 0$ and $x = L$, the boundary conditions for a given band i and a direction l are expressed as $I^+_{j,l,i,x=0} = a_{j,i,x=0} f_{i,x=0} I_{b,x=0}$ and $I^-_{j,l,i,x=L} = a_{j,i,x=L} f_{i,x=L} I_{b,x=L}$.

Once the radiative intensities of each spectral interval are determined, a summation has to be made over all spectral

ranges to obtain the total q_r and S_r:

$$q_r(x) = \sum_{i=1}^{n_b} \sum_{l=1}^{n_d} \sum_{j=1}^{J} 2\pi\mu_l\omega_l[I^+_{j,l,i}(x) - I^-_{j,l,i}(x)] \tag{11}$$

$$S_r(x) = \sum_{i=1}^{n_b} \sum_{l=1}^{n_d} \sum_{j=1}^{J} 2\pi\omega_l\kappa_j[I^+_{j,l,i}(x) + I^-_{j,l,i}(x)] - 4\pi\kappa_j a_{j,i} f_i I_b(x), \tag{12}$$

where n_b is the number of intervals in which the spectrum is divided. It is important to note that, in the equations above, the term f_i is included only in Eq. (12), since the blackbody intensity does not appear in the standard expression for q_r (Eq. (6)).

2.3 Problem description and solution methodology

The physical domain studied in the present paper consists of a 1D system bounded by two parallel infinite blacks walls, separated from each other by a distance $L = 1$ m, with the region between the plates filled with pure H_2O with a uniform molar concentration $Y = 0.2$, and under a total pressure $p = 1$ atm, that is depicted on the left side of Fig. 1. The spectral integration of the RTE is computed through the WBW model, whose methodology is proposed in the previous section. The domain is spatially discretized in 200 equal-sized cells and the directional integration of the RTE is performed with the DOM for 8 ordinates, adopting the set of weights and directional cosines presented in Lathrop and Carlson (1964). Complementary analyses showed that further refinements of the spatial and angular discretizations did not significantly affect the results.

To evaluate the accuracy of the WBW model against the LBL benchmark solution, the following two temperature profiles are tested:

$$T(\hat{x}) = 400 + 1400\sin^2(2\pi\hat{x}) \tag{13}$$

$$T(\hat{x}) = \begin{cases} 880 + 920\sin^2(2\pi\hat{x}), \text{if } \hat{x} \leq 0.25 \\ 400 + 1400\left\{1 - \sin^{3/2}[2\pi/3(\hat{x} - 0.25)]\right\}, \text{if } \hat{x} > 0.25 \end{cases}, \tag{14}$$

in which $\hat{x} = x/L$ is the dimensionless distance from the left plate. In Eq. (13) — referred as Profile 1 — a profile with double symmetry is presented, with both walls at 400 K and average temperature of the medium of 1100 K, reaching the maximum value of 1800 K in $\hat{x} = 0.25$ and $\hat{x} = 0.75$. Equation (14) — Profile 2 — describes an asymmetric profile, in which the temperature in the medium varies from 880 K at the left wall ($\hat{x} = 0$) to 1800 K at $\hat{x} = 0.25$, then decreases to 400 K at the right wall ($\hat{x} = 1.0$); the average temperature of the medium is also 1100 K. These temperature profiles are presented in the lower left part of Fig. 1.

In the next section, the results of radiative heat flux and radiative heat source include comparisons between the proposed methodology and the WSGG coefficients generated by other studies for pure water vapor. The central idea is to use the sets of coefficients generated for each spectral interval (more specifically, five regions for the test cases studied) under the assumption that the summation of the results found for q_r and S_r for all bands is equivalent to that obtained for the entire spectrum by applying the WSGG correlations presented in Cassol *et al.* (2014) and Coelho and França (2017), and by using the methodology proposed by Fonseca *et al.* (2020) for the GG model. To evaluate the accuracy of each one of the approaches studied here, a normalized percentage deviation from the reference solution is defined as

$$\Delta\phi = \frac{|\phi_{\text{ref}} - \phi_{\text{app}}|}{\max(|\phi_{\text{ref}}|)}, \tag{15}$$

where ϕ is either q_r or S_r, the subscripts "ref" and "app" are the reference and approximate solutions, respectively, and $\max(|\phi_{\text{ref}}|)$ is the maximum absolute local value of ϕ_{ref} in the domain.

3. RESULTS AND DISCUSSION

This section presents the emittances obtained with the division of the radiation spectrum into five segments following the criterion proposed by Marin and Buckius (1998) and according to the methodology discussed in Sections 2.2 and 2.3. Furthermore, the WBW coefficients for each spectral interval, as well as the results for the radiative heat flux and radiative heat source, are also presented and discussed in the next sections.

3.1 Determination of the emittances and coefficients for each spectral interval

From the absorption spectra of H_2O with $Y = 0.2$ and $p = 1$ atm, emittance data for each spectral interval $\Delta\eta$ selected are generated using Eq. (8), for 22 temperatures ranging from 400 K to 2500 K and 43 values of path-lengths from 0.001 m

to 30 m. Assuming the spectral range between 0 cm^{-1} to 25 000 cm^{-1} and following the procedures described in Section 2.2, the WBW coefficients are obtained via Eq. (9) for the five chosen spectral intervals (see Table 1 to know these ranges), each band with four gray gases (i.e., twenty gases in total). Table 1 presents the WBW coefficients for each one of the five spectral intervals studied in the present work.

Once the WBW coefficients are determined, the emittance values calculated with the proposed model can be obtained. Thus, from the coefficients obtained with the WBW model, the values of ε are calculated again and compared to those found directly from the LBL integration. Figure 2 shows a comparison between the emittances in function of the temperature obtained directly from the LBL data and those determined by the WBW coefficients presented in Table 1 for $S = 0.05$ m, $S = 0.5$ m, $S = 5$ m and $S = 30$ m, for the following spectral intervals: 0 $cm^{-1} < \eta < 1000$ cm^{-1}, 2600 $cm^{-1} < \eta < 4400$ cm^{-1} and 6000 $cm^{-1} < \eta < 25\,000$ cm^{-1}. For brevity, the emittances of all spectral ranges selected are not be shown — only the first, third and fifth bands (i.e., the spectral intervals 1000 $cm^{-1} < \eta < 2600$ cm^{-1} and 4400 $cm^{-1} < \eta < 6000$ cm^{-1} will be suppressed in this study, since these bands presented behaviors similar to those observed for the three intervals shown in Fig. 2; only the correlations obtained for these intervals will be presented, as shown in Table 1). For the same reason, only four values of path-lengths are being reported in Fig. 2, although the fits of the coefficients of the proposed model have been generated through calculations of emittance obtained with 43 values of $p_a S$.

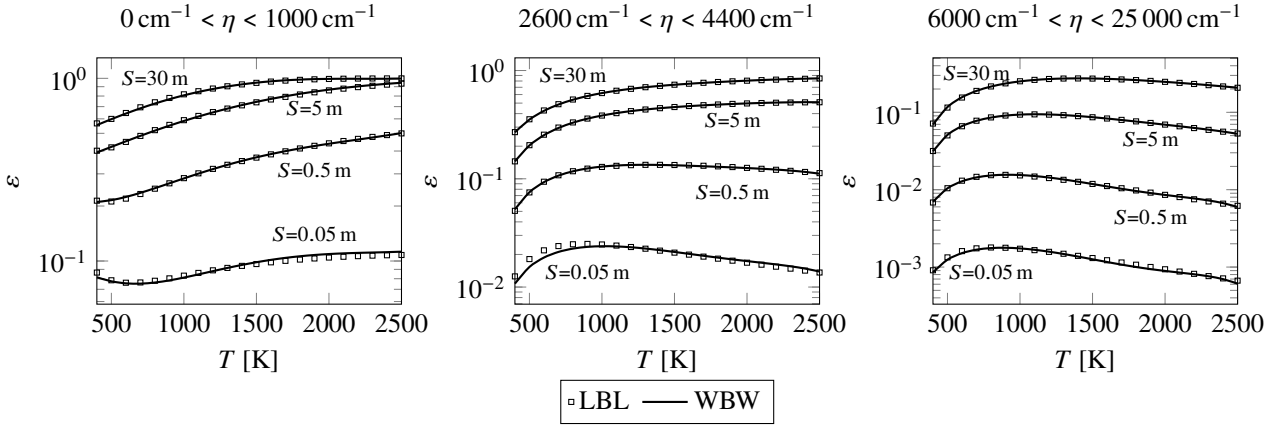

Figure 2. Comparison between the emittance computed by LBL and WBW solutions for three of the five analyzed spectral intervals.

As it can be seen in Fig. 2, the correlations generated through the WBW model provide a good fit of the emittance data obtained with the LBL solution for the entire range of temperatures and path-lengths for the three selected spectral intervals. In terms of the relative local deviations, $|\varepsilon_{\mathrm{LBL}} - \varepsilon_{\mathrm{WBW}}|/\varepsilon_{\mathrm{LBL}} \times 100$ %, the highest errors found are for the lowest path-length, $S = 0.05$ m, even for the omitted ranges in Fig. 2 (1000 $cm^{-1} < \eta < 2600$ cm^{-1} and 4400 $cm^{-1} < \eta < 6000$ cm^{-1}). For the spectral ranges shown in the figure, the largest relative deviations are 1.55 % and 0.43 % for the first and fifth bands, in the region with the highest temperatures, and 3.16 % for the third one, in the lowest temperature range, this being the biggest error found among all the analyzed ranges. Nevertheless, in the regions where the pressure path-length is low, the radiative heat transfer presents a minor importance for the solution of the problem, so that this error should not cause a major impact in global calculations.

3.2 Calculation of the radiative heat flux and radiative heat source

To assess the accuracy of the coefficients shown in Table 1, these correlations are applied to solve the radiative heat flux and radiative heat source for the two temperatures profiles studied in this paper (Eqs. (13) and (14)), through Eq. (15). Then, the WBW coefficients obtained with the proposed methodology and the WSGG coefficients generated by Cassol *et al.* (2014) and Coelho and França (2017) are employed to solve the domain of Fig. 1.

Figure 3(a) and Figure 3(b) present comparisons between the radiative heat flux and radiative heat source calculated through the LBL integration and the WBW method, in addition to the results obtained with the Cassol and Coelho correlations for Profile 1. According to the figure, satisfactory agreements between the approaches and the LBL method are observed, except for the solution with the GG model (i.e., Fonseca *et al.* (2020), with errors around 30 %), that, although it also uses a methodology that partitions the spectrum into five segments, it leads to noticeably large errors in relation to the reference solution. The maximum and average normalized deviations (subscripts "max" and "avg", respectively) for q_r and S_r computed with the different solutions discussed regarding LBL integration for all cases studied in this paper are shown in Table 2. By the table, one can note that the WBW model reduces by more than half the deviations when compared to the performance of the WSGG model with the correlations obtained by Cassol *et al.* (2014), with the maximum value of 6.65 % for S_r. Comparing the WBW model with the correlations of Coelho and França (2017) — both in relation to the LBL

Table 1. WBW coefficients for water vapor for $0\,\mathrm{cm}^{-1} \leq \eta \leq 25\,000\,\mathrm{cm}^{-1}$ and five spectral intervals.

j	κ_{pj} [$\mathrm{atm}^{-1}\,\mathrm{m}^{-1}$]	$b_{j,0}$	$b_{j,1}$ [K^{-1}]	$b_{j,2}$ [K^{-2}]	$b_{j,3}$ [K^{-3}]	$b_{j,4}$ [K^{-4}]
			$0\,\mathrm{cm}^{-1} < \eta < 1000\,\mathrm{cm}^{-1}$			
1	0.425	1.934×10^{-1}	1.092×10^{-4}	3.192×10^{-7}	-3.275×10^{-10}	6.889×10^{-14}
2	2.746	-3.177×10^{-2}	5.345×10^{-4}	-5.645×10^{-7}	3.416×10^{-10}	-6.723×10^{-14}
3	14.830	1.006×10^{-1}	-1.267×10^{-4}	3.889×10^{-7}	-2.154×10^{-10}	4.006×10^{-14}
4	109.493	1.701×10^{-1}	-2.795×10^{-4}	2.732×10^{-7}	-1.051×10^{-10}	1.348×10^{-14}
			$1000\,\mathrm{cm}^{-1} < \eta < 2600\,\mathrm{cm}^{-1}$			
1	0.289	-4.049×10^{-2}	8.020×10^{-4}	-6.332×10^{-7}	2.389×10^{-10}	-3.251×10^{-14}
2	1.772	6.476×10^{-2}	2.412×10^{-4}	-1.041×10^{-7}	3.191×10^{-11}	-4.349×10^{-15}
3	7.879	9.621×10^{-2}	2.406×10^{-4}	-2.391×10^{-7}	9.872×10^{-11}	-1.603×10^{-14}
4	54.237	1.938×10^{-1}	-1.916×10^{-4}	6.627×10^{-8}	-8.664×10^{-12}	1.583×10^{-16}
			$2600\,\mathrm{cm}^{-1} < \eta < 4400\,\mathrm{cm}^{-1}$			
1	0.261	3.055×10^{-3}	6.505×10^{-4}	-4.350×10^{-7}	1.359×10^{-10}	-1.567×10^{-14}
2	1.449	-7.695×10^{-2}	3.325×10^{-4}	-7.429×10^{-8}	8.100×10^{-12}	2.261×10^{-16}
3	6.261	-9.270×10^{-2}	4.606×10^{-4}	-3.481×10^{-7}	1.192×10^{-10}	-1.701×10^{-14}
4	39.524	-5.165×10^{-2}	2.791×10^{-4}	-2.828×10^{-7}	1.097×10^{-10}	-1.503×10^{-14}
			$4400\,\mathrm{cm}^{-1} < \eta < 6000\,\mathrm{cm}^{-1}$			
1	0.148	-1.384×10^{-1}	6.185×10^{-4}	-1.934×10^{-7}	3.799×10^{-11}	-2.930×10^{-15}
2	0.716	-5.830×10^{-2}	3.197×10^{-4}	-2.561×10^{-7}	1.190×10^{-10}	-1.990×10^{-14}
3	2.606	-3.941×10^{-2}	1.863×10^{-4}	-1.154×10^{-7}	2.135×10^{-11}	-8.367×10^{-16}
4	11.945	-5.978×10^{-3}	8.655×10^{-5}	-1.145×10^{-7}	5.256×10^{-11}	-8.072×10^{-15}
			$6000\,\mathrm{cm}^{-1} < \eta < 25\,000\,\mathrm{cm}^{-1}$			
1	0.061	-9.576×10^{-2}	3.895×10^{-4}	1.773×10^{-7}	-1.794×10^{-10}	3.242×10^{-14}
2	0.412	-1.360×10^{-1}	5.489×10^{-4}	-3.793×10^{-7}	1.017×10^{-10}	-9.663×10^{-15}
3	1.880	-5.573×10^{-2}	2.673×10^{-4}	-2.699×10^{-7}	1.045×10^{-10}	-1.430×10^{-14}
4	9.355	-8.692×10^{-3}	5.703×10^{-5}	-7.097×10^{-8}	3.262×10^{-11}	-5.112×10^{-15}

solution —, the deviations drop by a third (16.43 % for S_r), which shows that the proposed method better predicts the heat transfer than other formulations in the literature.

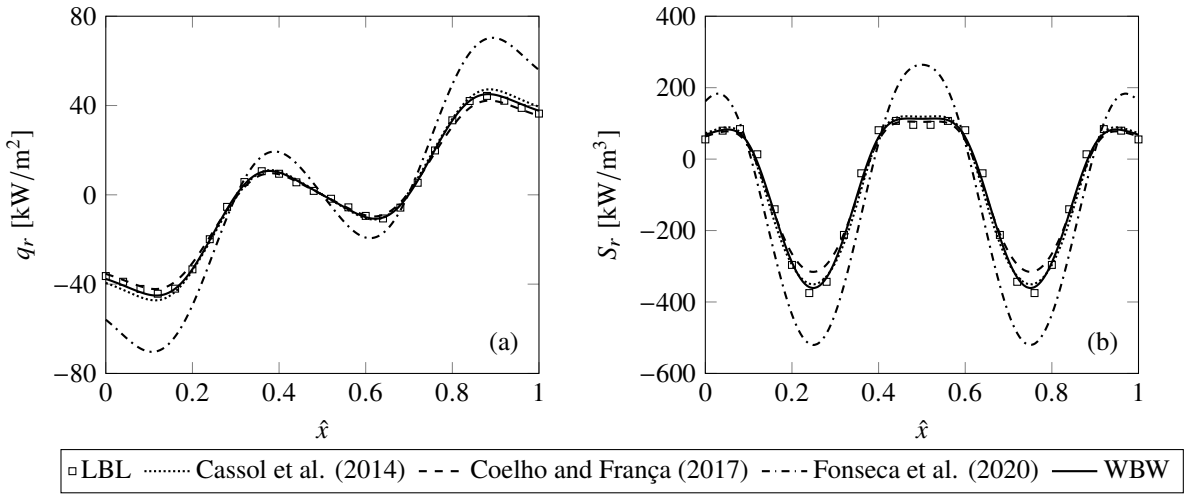

Figure 3. Radiative heat transfer for Profile 1: (a) radiative heat flux; (b) radiative heat source.

Figure 4(a) and Figure 4(b) show q_r and S_r for Profile 2, Eq. (14). Similar to what was observed with the previous case,

the approach of Fonseca *et al.* (2020) has the worst performance compared to other formulations, since the deviations are of the order of 25 % compared to the LBL solution. Again, the proposed methodology leads to the smallest errors for both the average and maximum deviations: the errors fell in half for the WBW model, showing that the proposed approach is more accurate, since the maximum error found was 7.24 % for S_r against 12.17 % and 15.63 % with the coefficients of Cassol *et al.* (2014) and Coelho and França (2017), respectively.

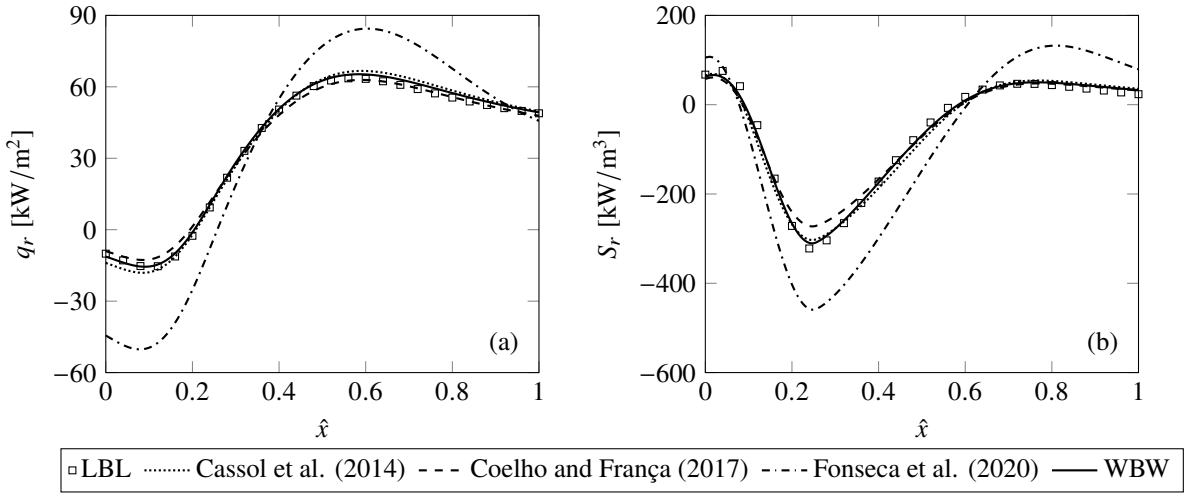

Figure 4. Radiative heat transfer for Profile 2: (a) radiative heat flux; (b) radiative heat source.

Table 2. Maximum and average normalized deviations predicted by the reference solution and the different approaches.

	LBL x Cassol et al. (2014) [%]				LBL x Coelho and França (2017) [%]				LBL x WBW [%]			
Profile	$(\Delta q_r)_{\max}$	$(\Delta q_r)_{\text{avg}}$	$(\Delta S_r)_{\max}$	$(\Delta S_r)_{\text{avg}}$	$(\Delta q_r)_{\max}$	$(\Delta q_r)_{\text{avg}}$	$(\Delta S_r)_{\max}$	$(\Delta S_r)_{\text{avg}}$	$(\Delta q_r)_{\max}$	$(\Delta q_r)_{\text{avg}}$	$(\Delta S_r)_{\max}$	$(\Delta S_r)_{\text{avg}}$
1	8.46	4.02	11.88	5.46	7.24	3.13	16.43	6.13	3.72	1.70	6.65	3.39
2	6.13	3.05	12.17	4.26	6.96	2.18	15.62	4.54	3.50	1.83	7.25	2.49

4. CONCLUSIONS

In this paper, a study was carried out on the problem of radiative heat transfer in a 1D system bounded by two infinite parallel black plates, in which the participating medium is filled with a homogeneous concentration of H_2O. A methodology of a new spectral model, that is an adaptation of the standard WSGG model, was proposed, in which the radiation spectrum was divided into five segments following recommendations from previous studies and four gray gases were distributed in each one of these intervals. The emittance data and the WBW coefficients showed a satisfactory fit compared to the LBL benchmark solution. For the test cases studied, the results for the radiative heat flux and radiative heat source presented a good agreement in relation to the LBL method and also in comparison with other approaches in the literature for the WSGG model. For S_r, which was the physical quantity that presented the largest deviations for the cases tested in this paper, the errors in relation to the LBL solution reduced of the order of 15 % to 5 %, which shows an indisputable improvement compared to the results found with other formulations of the WSGG model in the literature. For future studies, a possible proposal for the continuity of the work is to generate correlations for other pure chemical species, such as CO, CO_2 and CH_4, and also for mixtures of water vapor and carbon dioxide with soot. Another likely way is to increase the number of divisions of the spectrum and optimize the amount of gray gases in each spectrum range, in order to obtain the best result with the least number of gases possible to make the model competitive in relation to other formulations with only four gases for the entire spectrum.

5. ACKNOWLEDGMENTS

This work has been partially supported by the Brazilian Agency CAPES (Coordenação de Aperfeiçoamento de Pessoal de Nível Superior). Authors RJCF and FRC thank CAPES for doctorate scholarships. Authors GCF and FHRF thank CNPq (Conselho Nacional de Desenvolvimento Tecnológico e Científico) for postdoctoral scholarship and research grant 302686/2017-7.

6. REFERENCES

Bordbar, H., Coelho, F.R., Fraga, G.C., França, F.H. and Hostikka, S., 2021. "Pressure-dependent weighted-sum-of-gray-gases models for heterogeneous CO_2-H_2O mixtures at sub- and super-atmospheric pressure". *International Journal of Heat and Mass Transfer*, Vol. 173, p. 121207.

Brittes, R., Centeno, F.R., Ziemniczak, A. and França, F.H.R., 2017. "WSGG model correlations to compute nongray radiation from carbon monoxide in combustion applications". *Journal of Heat Transfer*, Vol. 139, No. 4, p. 041202.

Cassol, F., Brittes, R., Centeno, F.R., da Silva, C.V. and França, F.H., 2015. "Evaluation of the gray gas model to compute radiative transfer in non-isothermal, non-homogeneous participating medium containing CO_2, H_2O and soot". *Journal of the Brazilian Society of Mechanical Sciences and Engineering*, Vol. 37, No. 1, pp. 163–172.

Cassol, F., Brittes, R., França, F.H. and Ezekoye, O.A., 2014. "Application of the weighted-sum-of-gray-gases model for media composed of arbitrary concentrations of H_2O, CO_2 and soot". *International Journal of Heat and Mass Transfer*, Vol. 79, pp. 796–806.

Centeno, F.R., Brittes, R., Rodrigues, L.G., Coelho, F.R. and França, F.H., 2018. "Evaluation of the WSGG model against line-by-line calculation of thermal radiation in a non-gray sooting medium representing an axisymmetric laminar jet flame". *International Journal of Heat and Mass Transfer*, Vol. 124, pp. 475–483.

Chandrasekhar, S., 1960. *Radiative Transfer*. Dover Publications.

Coelho, F.R. and França, F.H., 2018. "WSGG correlations based on HITEMP2010 for gas mixtures of H_2O and CO_2 in high total pressure conditions". *International Journal of Heat and Mass Transfer*, Vol. 127, pp. 105–114.

Coelho, F.R. and França, F.H.R., 2017. "WSGG correlations for H_2O and CO_2 in high pressure conditions". In *Proceedings of the 24th ABCM International Congress of Mechanical Engineering*. ABCM.

Denison, M.K. and Webb, B.W., 1993. "A spectral line-based weighted-sum-of-gray-gases model for arbitrary RTE solvers". *Journal of Heat Transfer*, Vol. 115, No. 4, pp. 1004–1012.

Dorigon, L.J., Duciak, G., Brittes, R., Cassol, F., Galarça, M. and França, F.H.R., 2013. "WSGG correlations based on HITEMP2010 for computation of thermal radiation in non-isothermal, non-homogeneous H_2O/CO_2 mixtures". *International Journal of Heat and Mass Transfer*, Vol. 64, pp. 863–873.

Fonseca, R.J.C., Fraga, G.C. and França, F.H.R., 2020. "A wide-band formulation based on the gray gas model applied to non-isothermal and homogeneous water vapor media". In *Procceedings of the 18th Brazilian Congress of Thermal Sciences and Engineering*. ABCM.

Fraga, G., Zannoni, L., Centeno, F. and França, F., 2019. "Evaluation of different gray gas formulations against line-by-line calculations in two- and three-dimensional configurations for participating media composed by CO_2, H_2O and soot". *Fire Safety Journal*, Vol. 108, p. 102843.

Gordon, I.E., Rothman, L.S., Hill, C., Babikov, Y., Barde, A., Chris Benner, D., Bernath, P.F., Birk, M., Bizzocchi, L., Boudon, V., Brown, L.R., Campargue, A., Chance, K., Cohen, E.A., Coudert, L.H., Devi, V.M., Drouin, B.J., Fayt, A., Flaud, J.M., Gamache, R.R., Harrison, J.J., Hartmann, J.M., Hodges, J.T., Jacquemart, D., Jolly, A., Lamouroux, J., Le Roy, R.J., Li, G., Long, D.A., Lyulin, O.M., Mackie, C.J., Massie, S.T., Mikhailenko, S., Müller, H.S.P., Naumenko, O.V., Nikitin, A.V., Orphal, J., Perevalov, V., Perrin, A., Polovtseva, E.R., Richard, C., Smith, M.A.H., Starikova, E., Sung, K., Tashkun, S., Tennyson, J., Toon, G.C., Tyuterev, V.G. and Wagner, G., 2017. "The HITRAN2016 molecular spectroscopic database". *Journal of Quantitative Spectroscopy and Radiative Transfer*, Vol. 203, pp. 3–69.

He, Z., Dong, C., Liang, D. and Mao, J., 2021. "A weighted-sum-of-gray soot-fractal-aggregates model for nongray heat radiation in the high temperature gas-soot mixture". *Journal of Quantitative Spectroscopy and Radiative Transfer*, Vol. 260, p. 107431.

Hottel, H.C. and Sarofim, A.F., 1967. *Radiative Transfer*. McGraw-Hill.

Howell, J.R., Mengüç, M.P. and Siegel, R., 2016. *Thermal Radiation Heat Transfer*. CRC press, 6th edition.

IBM, 2016. *IBM SPSS Modeler 18.0 User's Guide*. IBM Corporation.

Kangwanpongpan, T., França, F.H.R., da Silva, R.C., Schneider, P.S. and Krautz, H.J., 2012. "New correlations for the weighted-sum-of-gray-gases model in oxy-fuel conditions based on HITEMP 2010 database". *International Journal of Heat and Mass Transfer*, Vol. 55, No. 25, pp. 7419–7433.

Lathrop, K.D. and Carlson, B.G., 1964. "Discrete ordinates angular quadrature of the neutron transport equation".

Marin, O. and Buckius, R., 1998. "A simplified wide band model of the cumulative distribution function for water vapor". *International Journal of Heat and Mass Transfer*, Vol. 41, No. 19, pp. 2877–2892.

Marquardt, D.W., 1963. "An algorithm for least-squares estimation of nonlinear parameters". *Journal of the Society for Industrial and Applied Mathematics*, Vol. 11, No. 2, pp. 431–441.

Modest, M.F., 2013. *Radiative Heat Transfer*. Academic Press.

Modest, M.F. and Zhang, H., 2000. "The full-spectrum correlated-k distribution and its relationship to the weightd-sum-of-gray-gases method". In *Proceedings of IMECE2000*.

Mossi, A., Galarça, M.M., Brittes, R., Vielmo, H.A. and França, F.H.R., 2012. "Comparison of spectral models in the computation of radiative heat transfer in participating media composed of gases and soot". *Journal of the Brazilian*

Society of Mechanical Sciences and Engineering, Vol. 34, No. 2, pp. 112–119.

Rothman, L., Gordon, I., Barber, R., Dothe, H., Gamache, R., Goldman, A., Perevalov, V., Tashkun, S. and Tennyson, J., 2010. "HITEMP, the high-temperature molecular spectroscopic database". *Journal of Quantitative Spectroscopy and Radiative Transfer*, Vol. 111, No. 15, pp. 2139–2150.

Solovjov, V.P. and Webb, B.W., 2002. "A local-spectrum correlated model for radiative transfer in non-uniform gas media". *Journal of Quantitative Spectroscopy and Radiative Transfer*, Vol. 73, No. 2-5, pp. 361–373.

Taine, J., 1983. "A line-by-line calculation of low-resolution radiative properties of CO_2-CO-transparent nonisothermal gases mixtures up to 3000 K". *Journal of Quantitative Spectroscopy and Radiative Transfer*, Vol. 30, No. 4, pp. 371–379.

Wang, B. and Xuan, Y., 2019. "An improved WSGG model for exhaust gases of aero engines within broader ranges of temperature and pressure variations". *International Journal of Heat and Mass Transfer*, Vol. 136, pp. 1299–1310.

7. RESPONSIBILITY NOTICE

The authors are solely responsible for the printed material included in this paper.